

Spectral characteristics of an injection-controlled XeF($C \rightarrow A$) excimer laser

C. B. Dane, S. Yamaguchi, Th. Hofmann, R. Sauerbrey, W. L. Wilson, and F. K. Tittel
Rice University, Department of Electrical and Computer Engineering, Houston, Texas 77251-1892

(Received 4 December 1989; accepted for publication 16 April 1990)

The spectral output characteristics of an injection-controlled XeF($C \rightarrow A$) excimer laser pumped by a short pulse (10 ns), high current density (250 A/cm²) electron beam are reported. A tuning bandwidth of 50 nm full width half maximum, centered at 490 nm, with a peak specific energy density of 1.3 J/ℓ was measured using an injection laser intensity of ~ 2 MW/cm². Continuously tuned output across the entire blue-green region (450–530 nm) with an energy density exceeding 0.2 J/ℓ was achieved. Injection beam spectral linewidths as narrow as 0.001 nm were shown to be preserved in the XeF($C \rightarrow A$) laser output.

The XeF($C \rightarrow A$) transition has a unique broadband spectrum in the blue-green. When the XeF($C \rightarrow A$) excimer laser is operated as a free-running oscillator, the output is centered at 485 nm with a typical spectral width of 15–20 nm.^{1–3} The use of a short, intense electron beam as an excitation source results in peak gains of $\sim 3\%$ /cm allowing the laser to be effectively injection controlled with a relatively low-power injection beam. With this technique, narrowband operation across the spectral gain profile has been previously demonstrated between 470 and 500 nm.⁴ Recent XeF($C \rightarrow A$) electron beam pumped laser scaling experiments have been performed in which the active laser volume was increased to 0.50 ℓ from that of 0.02 ℓ used in the experiments described in Ref. 4. Using a kinetically tailored gas mixture composed of F₂, NF₃, Xe, Kr, and Ar,⁵ a specific energy density of 1.5 J/ℓ and an intrinsic efficiency of 1.2% were achieved at 486.8 nm, corresponding to an output energy of 0.7 J.⁶ In this letter the tuning performance of the scaled XeF($C \rightarrow A$) laser system, excited by a short (10 ns), intense (~ 10 MW/cm³) electron beam is reported for the extended wavelength region between 450 and 530 nm.

The electron beam pumped laser system used for these experiments has been described in detail elsewhere.^{6–8} The active laser medium was 3.5 cm in diameter and 50 cm in length, corresponding to a volume of ~ 0.5 ℓ. The average electron beam energy deposition into this volume was measured to be 120 J/ℓ using chlorostyrene film dosimetry.⁹ The injection source was a grating tuned excimer pumped dye laser (Lambda Physik FL3002) with a bandwidth of ~ 0.005 nm at 480 nm (6 GHz) and a temporal pulse width of ~ 40 ns full width half maximum (FWHM). By installing an intracavity étalon, the bandwidth could be reduced to ~ 0.001 nm (1.5 GHz) for the same wavelength. The optimized laser gas mixture was composed of 12 Torr NF₃, 1 Torr F₂, 12 Torr Xe, and 750 Torr Kr and was completed to a total pressure of 6.5 bar with an Ar buffer.⁸

A positive branch confocal unstable resonator with a magnification of 1.34 was chosen for these experiments. Analytical modeling of the injection control process^{10,11} indicated that a reduction in cavity magnification from the predicted optimum near 2 would not lead to a significant

reduction in output energy at the center of the spectral gain profile. The smaller output coupling of this configuration, however, was expected to improve laser performance in the low gain regions, away from the wavelength peak of the transition. The concave resonator mirror, with a radius of curvature of 4.57 m, had a 1.5-mm-diam masked spot centered on the reflective coating through which the injection beam entered the resonator. The output coupler was a double meniscus lens with radii of curvature of ± 3.42 m and had a 26-mm-diam high reflectivity spot centered on the convex surface. Three optics sets with different optical coatings were used to maintain $> 99\%$ reflectivity over the entire XeF($C \rightarrow A$) laser bandwidth (see Fig. 1).

The XeF($C \rightarrow A$) laser output energy was monitored by a pyroelectric energy meter and the temporal pulse duration, typically 10 ns FWHM, was measured using a vacuum photodiode. The wavelength spectrum of the laser output was recorded using an optical multichannel analyzer (OMA) spectrometer with a resolution of 0.2 nm. To measure the spectral bandwidth of the output of the injection dye laser and of the electron beam pumped amplifier, an air spaced plane-plane étalon was used with a finesse of 30 and a free spectral range of either 9 or 30 GHz. The output beam was focused using a planoconvex lens with a 50 cm focal length onto an opal glass diffuser which was placed in front of the étalon. The resulting circular interference pattern was imaged onto a two-dimensional charge-coupled device (CCD) array by a 30 cm focal length planoconvex lens.

The output energy of the injection-controlled XeF($C \rightarrow A$) laser was measured at selected wavelengths across the transition bandwidth. At each wavelength, measurements were made using the maximum injection intensity available from the dye laser injection source as well as 1/10 and 1/100 of that intensity. Typically, a maximum laser intensity of ~ 4 MW/cm², corresponding to a dye laser pulse energy of ~ 3 mJ, could be coupled through the 1.5 mm injection aperture at the peak wavelength for each dye. However, in order to compare the laser performance across the entire bandwidth at a constant injection intensity, the output energy at each wavelength was predicted for an normalized injection intensity of 2 MW/cm² (~ 1.5 mJ) by interpolation. To achieve this intensity across the

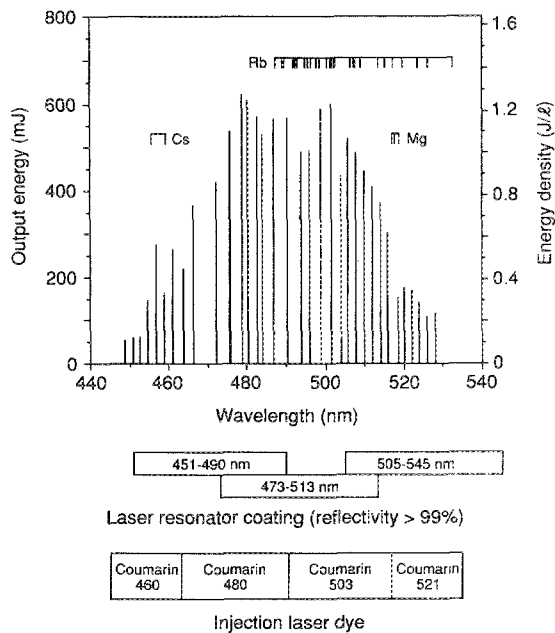


FIG. 1. Output energies for the injection-controlled XeF($C \rightarrow A$) laser between 450 and 530 nm showing a tuning bandwidth of 50 nm FWHM centered at 490 nm. The dye laser injection intensity was 2 MW/cm^2 with a spectral linewidth of 0.005 nm. The wavelengths shown were chosen not to coincide with narrow-band atomic absorptions occurring in this spectral region. Three different resonator coatings and four injection laser dyes were used to span the XeF($C \rightarrow A$) tuning bandwidth.

XeF($C \rightarrow A$) spectral gain region, four different Coumarin dyes were used in the dye laser injection source (see Fig. 1). Also, the laser system was observed to be highly sensitive to the broadband amplified spontaneous emission (ASE) content of the dye laser output ($\sim 1\%$) requiring that the injection wavelength be near the center of the bandwidth of the dye in use.

Shown in Fig. 1 is the output energy of the XeF($C \rightarrow A$) injection-controlled laser for wavelengths between 450 and 530 nm chosen not to coincide with known narrowband atomic absorptions. The injection dye laser had a linewidth of 0.005 nm and the data were normalized to an injection intensity of 2 MW/cm^2 . A tuning bandwidth of $\sim 50 \text{ nm}$ (FWHM), centered at 490 nm, was observed for this injection intensity with a peak specific energy density of 1.3 J/ℓ . A maximum laser output of 0.7 J was measured at 486.8 nm using an injection intensity of 4 MW/cm^2 , corresponding to an energy density of 1.4 J/ℓ and an intrinsic efficiency of 1.2%. Even in the wings of the gain profile, at 450 and 530 nm, an energy density of 0.2 J/ℓ was obtained with complete spectral control of the laser output. Also indicated in Fig. 1 are the four injection laser dyes and three resonator coatings used to span the XeF($C \rightarrow A$) spectral gain region.

When the XeF($C \rightarrow A$) laser is operated as a free-running oscillator, the output spectral profile is not smooth across the $\sim 20 \text{ nm}$ output bandwidth but is characterized by strong dips that result from discrete, narrow-band absorptions. These are attributed to transitions in excited rare-gas atoms present in the laser gas mixture. The effect

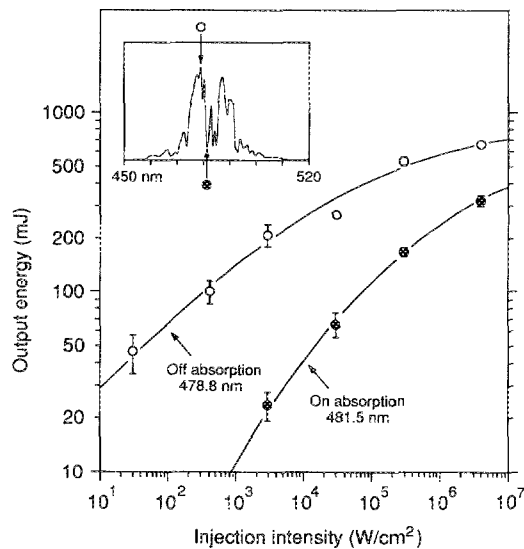
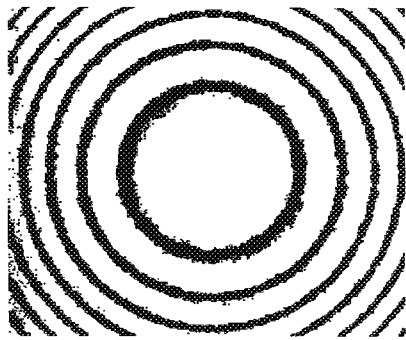


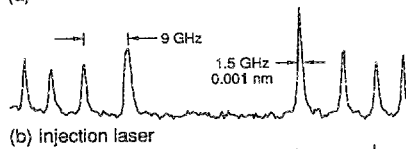
FIG. 2. Dependence of injection controlled XeF($C \rightarrow A$) laser output energy on injection intensity. The outputs were measured for a wavelength in coincidence (481.5 nm, filled circles) and not in coincidence (478.8 nm, open circles) with a narrow-band background absorption as illustrated by the inset of the free-running laser spectrum. The ratio of output energy at the peak wavelength to that at the valley wavelength decreased from a factor of ~ 10 at 30 kW/cm^2 to only ~ 2 at an injection intensity of 4 MW/cm^2 . For the 40 ns FWHM dye laser injection pulses used, an intensity of 4 MW/cm^2 corresponded to an energy of $\sim 3 \text{ mJ}$ delivered through the injection aperture.

of these absorptions was significantly reduced in the injection-controlled XeF($C \rightarrow A$) laser. Selected wavelengths were chosen to coincide with peak and valley structures in the free-running spectrum. For an injection intensity of 2 MW/cm^2 , the laser output was generally reduced less than 50% when tuned in coincides with these narrow-band absorbers. Gain measurements have shown that this improvement in the valley positions is the result of the saturation of these absorptions by the laser photon flux.⁴ By choosing relatively closely spaced peak (478.8 nm) and valley (481.5 nm) wavelengths, the effect of this saturation was demonstrated. Figure 2 shows the injection-controlled laser output at these two wavelengths for injection intensities ranging between 30 kW/cm^2 and 4 MW/cm^2 . For injection intensities below $\sim 1 \text{ kW/cm}^2$, no measurable output is observed at 481.5 nm. The ratio of output at 478.8 nm to that at 481.5 nm decreases from ~ 10 at 30 kW/cm^2 to only ~ 2 at 4 MW/cm^2 . Extrapolation of these measured curves suggests that this ratio should be even further reduced at higher injection intensities.

Figure 3(a) shows the circular interference pattern generated from a monitor étalon with a 9 GHz FSR using a laser bandwidth of 0.001 nm. Figure 3(b) is a horizontal cross section of this pattern for the output of the injection laser source at 486.8 nm. When this injection signal was used to injection control the XeF($C \rightarrow A$) amplifier, the interference pattern in Fig. 3(c) resulted, showing complete preservation of the injection laser linewidth and wavelength to within the resolution of the CCD detector. Similar results were recorded with a laser bandwidth of



(a)



(b) injection laser



(c) Amplified XeF(C→A) output

FIG. 3. (a) A circular interference pattern, for a laser linewidth of 0.001 nm, captured by a CCD array using a monitor étalon with a FSR of 9 GHz. (b) A horizontal cross section of the interference pattern generated using the injection dye laser output. (c) Interference pattern of the amplified XeF(C→A) laser output showing preservation of input wavelength and spectral bandwidth. Similar results were measured for an injection linewidth of 0.005 nm.

0.005 nm using a monitor étalon with a FSR of 30 GHz. When the injection linewidth was decreased from 0.005 to 0.001 nm, no measurable decrease in laser output energy was observed resulting in a fivefold increase in spectral brightness.

In conclusion, the wavelength tunability of an injection-controlled XeF(C→A) electron beam pumped laser was demonstrated across the entire blue-green region of the spectrum. A tuning bandwidth of 50 nm (FWHM) with a peak specific energy density of 1.3 J// was observed using an injection intensity of 2 MW/cm². The experimental results show that the XeF(C→A) spectral gain region, extending between 450 and 530 nm, was fully available as narrow-band injection-controlled output using the high current density electron beam pumped device. The spectral

bandwidth of the tuned output from the XeF(C→A) laser was found to completely preserve that of the injection dye laser for linewidths as narrow as 0.001 nm. As illustrated in Fig. 1, the accessible spectral region includes the wavelength of various atomic resonance filters^{12,13} and overlaps the window of maximum transmission of water.¹⁴ These results make the XeF(C→A) laser an attractive candidate for applications requiring high-power wavelength tunability, and spectral bandwidth control such as those in optical communications and remote sensing. In addition, the broad transition bandwidth, which is larger than those available from organic dyes, makes the XeF(C→A) system an excellent candidate for the amplification of ultrashort laser pulses in the blue green.

We would like to acknowledge the technical assistance of J. R. Hooten of Rice University. Helpful comments by W. L. Nighan of United Technologies Research Center (UTRC) are sincerely appreciated. We would also like to thank R. A. Rubino of UTRC for the loan of the monitor étalon. This work was supported by the Office of Naval Research, the Robert Welch Foundation, and the National Science Foundation.

¹A. Mandl and L. H. Litzenger, *Appl. Phys. Lett.* **53**, 1690 (1989).

²D. J. Eckstrom and H. C. Walker, *IEEE J. Quantum Electron.* **18**, 176 (1982).

³W. L. Nighan, F. K. Tittel, W. L. Wilson, N. Nishida, Y. Zhu, and R. Sauerbrey, *Appl. Phys. Lett.* **45**, 947 (1984).

⁴N. Hamada, R. Sauerbrey, W. L. Wilson, F. K. Tittel, and W. L. Nighan, *IEEE J. Quantum. Electron.* **24**, 1571 (1988).

⁵W. L. Nighan and M. C. Fowler, *IEEE J. Quantum Electron.* **25**, 791 (1989).

⁶G. J. Hirst, C. B. Dane, W. L. Wilson, R. Sauerbrey, F. K. Tittel, and W. L. Nighan, *Appl. Phys. Lett.* **54**, 1851 (1989).

⁷S. Lloyd, Y. G. Chen, G. McAllister, M. Montgomery, T. Olson, J. Shannon, B. Dane, G. Hirst, R. Sauerbrey, F. Tittel, and W. Wilson, *Proceedings of the Seventh IEEE Pulsed Power Conference*, Monterey, CA, 1989.

⁸C. B. Dane, G. J. Hirst, S. Yamaguchi, Th. Hofmann, W. L. Wilson, R. Sauerbrey, F. K. Tittel, W. L. Nighan, and M. C. Fowler, *Special Issue on Electronic Transitions Gas Lasers*, September, 1990, *IEEE J. Quantum. Electron.* (to be published).

⁹W. P. Bishop, K. C. Humpherys, and P. T. Randike, *Rev. Sci. Instrum.* **44**, 443 (1973).

¹⁰N. Hamada, R. Sauerbrey, and F. K. Tittel, *IEEE J. Quantum Electron.* **24**, 2458 (1988).

¹¹C. B. Dane, Th. Hofmann, G. J. Hirst, S. Yamaguchi, R. Sauerbrey, and F. K. Tittel, *IEEE J. Quantum. Electron.* (to be published).

¹²J. A. Gelbwachs, *IEEE J. Quantum. Electron.* **24**, 1266 (1988).

¹³T. M. Shay and Yun C. Chung, *Opt. Lett.* **13**, 443 (1988).

¹⁴W. L. Wolfe and G. J. Zissis, *The Infrared Handbook* (Office of Naval Research, Washington, DC, 1978), pp. 3-107.